

END TO END MULTIPARTICLE SIMULATIONS OF THE AIRIX LINAC

N. Pichoff*, A. Compant-La-Fontaine, Bruyères-le-Châtel, France

Abstract

AIRIX is a working 3 kA, 20 MeV induction accelerator. It has been designed with an envelope code : ENV. A new set of multiparticle codes (PBGUNS, MAGIC, PARMELA and PARTRAN) has been used recently to simulate the beam transport with an higher accuracy especially taking into account the field non-linearities. A dedicated space-charge routine has been written. The calculation results have been compared to experimental measurements.

INTRODUCTION

AIRIX accelerator is providing high flux short X-rays pulses for radiography purpose. The X-ray pulse is produced from a high current (2 kA), 20 MeV, short (70 ns) electron pulse colliding a Tantalum target. The beam is produced on a velvet cathode in a 4 MV pulsed diode and accelerated through induction cells to its maximum energy. It is then focused on the target with a solenoid. From now, the beam dynamics was calculated with an 1D envelope code ENV [1]. Even if it is very efficient to help users to tune the linac, it is unable to estimate the correct size of the focal spot on the target. Moreover, the input data used by ENV have been obtained from experimental measurements, using some restrictive assumptions, which prevent from easily evaluating new configurations. For example, the assumption that the beam has its full energy at the anode position is made, as, in reality, the fringe field of the diode continues to accelerated the beam downstream the anode. We have then decided to build up a set of codes whose goal is to be able to simulate the accelerator from cathode to target, and to predict the focal spot size. The accelerator is then divided in 3 parts which can be simulated independently and couple together :

- The diode where electrons are produced on a velvet cathode and accelerated to 3,85 MeV in about 20 cm. The steady state is simulated with PBGUNS [2] code, and the full pulse (including transient) with MAGIC [3] codes. The results are compared to experimental measurement.
- The accelerator is simulated with PARTRAN [4] codes. Particle distributions from PBGUNS and MAGIC can be used at PARTRAN input. PARTRAN is assuming continuous beam as the pulse length is much longer than beam transverse size.
- The final focusing is simulated by coupling the M2V [5] code solving Maxwell equations and the VAPOR [6] code calculating the target evaporation and ionisation under the electron beam impact.

DIODE SIMULATION

The geometry of the simulated diode, with a zoom on the cathode, is plotted on figure 1. The beam is produced on the cathode under space-charge limited flow. One solenoid is used to focused the beam out of the diode, an other is used to cancel the magnetic field on the cathode. The beam currents predicted by both PBGUNS and MAGIC are the same (1.70 kA, with a 3.96 MV voltage), but are slightly lower than this experimentally measured (1.92 kA). The reason have not been understood completely for the moment. However, changing the size of the cathode in the simulations to get 1.92 kA does not change significantly the beam characteristics at the position of the anode.

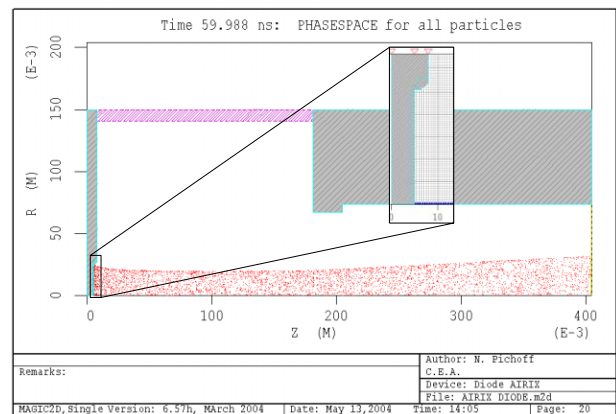


Figure 1: Diode simulated geometry.

Despite the very different model used by both codes, the beam distributions in (x, x') phase-space at anode level in the stationary conditions (excluded front edges) obtained with both codes are very similar (figure 2).

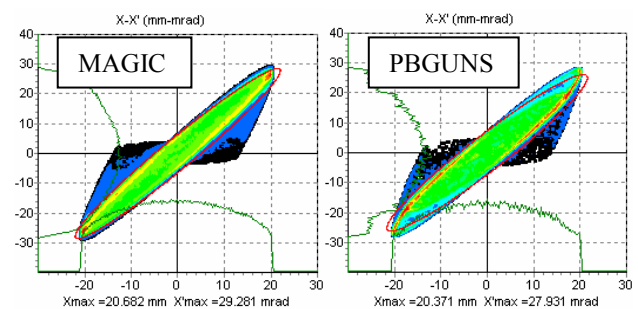


Figure 2 : Beam (x, x') distribution at anode level.

These distributions are injected at input of PARTRAN code to transport the beam about 1.7 m downstream where its size has been measured experimentally for varying solenoid strength. In PARTRAN, the beam

* nicolas.pichoff@cea.fr

current has been set to 1.92 kA to fit the measured one. The evolution of the beam size with the solenoid current (strength) is plotted on figure 3. The agreement between codes and experimental results is "acceptable". The experimental size has been measurement by triggering the camera at the middle of the pulse.

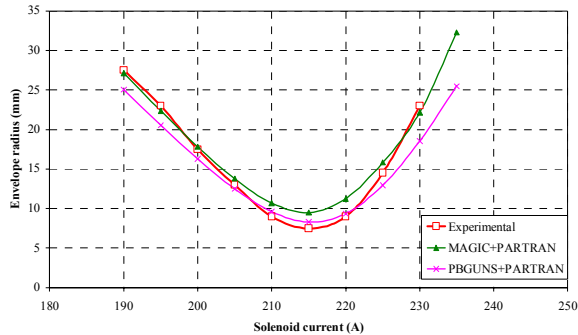


Figure 3 : DC photo-injector schematic layout.

LINAC SIMULATION

The beam is injected at anode level and transported to the end of the linac. The inductive cells are modelled with electrostatic field maps given by expression in [7]. The solenoid are modelled by magnetic field map fitted from experimental field measurement [8].

SCAIRIX, a new space-charge routine

The space-charge routine usually used in PARTRAN for axi-symmetric beam is based on the very famous LANL SCHEFF routine used in PARMELA [9] or PARMILA [10]. This routine is called PICNIR in PARTRAN as it has been re-written and modified in many aspects. Even if it is a very efficient routine, it is not perfectly matched for very high current continuous electron beams focused with solenoid. For this reason, we have developed a space-charge routine dedicated to AIRIX called SCAIRIX. This routine deals with continuous axi-symmetric beam and takes into account effects of diamagnetism* observed in solenoids. It also copes with the effect on the energy change† of converging or diverging beams and the change of pipe radius.

The envelope between simulations with PICNIR and SCAIRIX in the first 2 meters has been plotted on figure 4. The difference is significant and has a non-negligible influence on the simulation in the full linac. By suppressing from SCAIRIX effects not taken into account in PICNIR, i.e. diamagnetism and effects of varying size and vacuum chamber radius on beam energy (called "SCAIRIX-simul PICNIR" on the figure), the result is very close from this obtained with PICNIR.

* The solenoid gives rotation to the beam. This rotation induced longitudinal magnetic field that partly cancels the solenoid magnetic field.

† The density increasing gradient of a converging beam induced an decelerating electric field. An increase of beam pipe also induces an decelerating electric field.

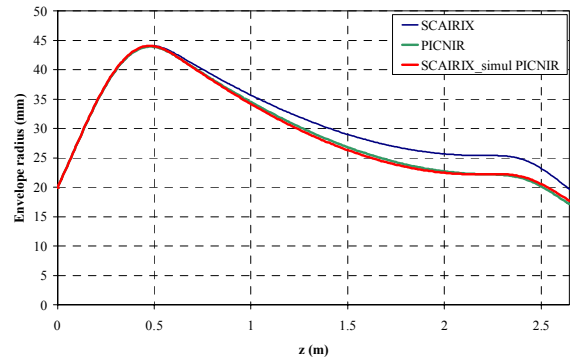


Figure 4: DC photo-injector schematic layout.

The simulation results obtained with PARTRAN +SCAIRIX are very close to these given by ENV in the same conditions (no more acceleration at anode, KV input beam).

The beam envelope in the linac is given on figure 5. The beam is mismatched and 100% emittance growth is observed. However, the exact beam energy out of the diode is not perfectly known for the moment and would be probably a little bit lower than this used in the calculations, which would improve the beam matching to the linac.

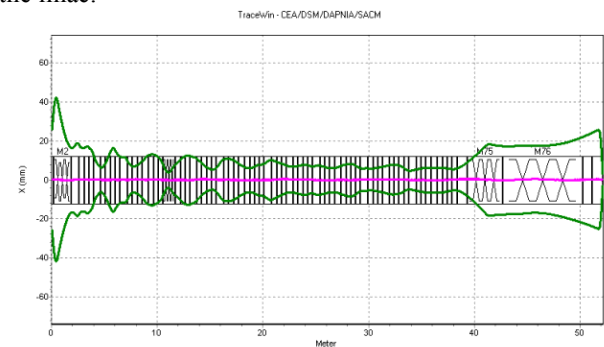


Figure 5 : DC photo-injector schematic layout.

The beam phase-space distribution on the cathode is presented on figure 6. The beam envelope diameter is about 0.7 mm, which is much smaller than the measured X-ray spot size.

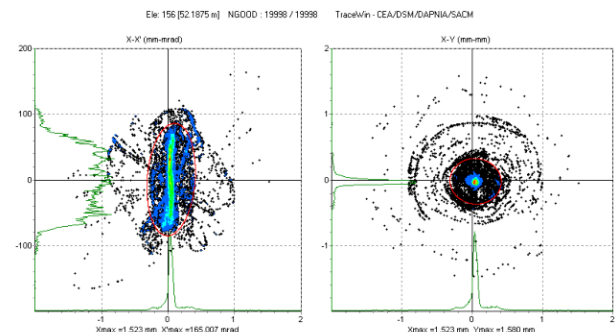


Figure 6 : Beam phase-space on the target.

In order to reproduce the correct beam size, a other effects have to be taken into account. The interaction between the

target and the beam is suspected as being the most relevant.

BEAM-TARGET INTERACTION

Two codes have been used to calculate the beam interaction on the target. The input electron beam is KV with constant parameters with time except its current (10 ns rise-time and fall times and 70 ns plateau are considered). The first code, M2V, calculates particle transport and solves Maxwell equations. It is firstly used to transport the electron pulse front edge to the target. The obtained beam size and power deposition on a time step dt is used in a second code, VAPOR, that calculates the vaporisation and ionisation of a target atoms under electron beam impact. The created atoms are then injected in M2V which calculates the particles transport during the next dt and so on. The phenomenon is the following : When the sub-millimetric intense electron beam hits the target, the power deposition is so high (the beam power is about $2 \text{ kA} \times 20 \text{ MeV} = 40 \text{ GW}$) than the target surface is evaporated. The vaporised atoms are ionised and accelerated back stream by the beam and the associated field. These moving ions induces a very high focusing force on the beam which is over focused. Their acceleration in the axial electric field leads to an increase with time of the focal spot on the target (figure 7).

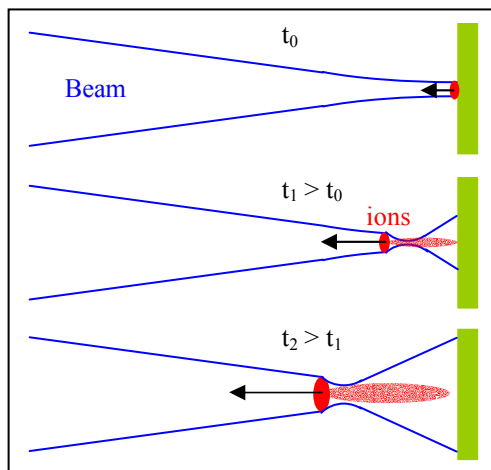


Figure 7: Schematic of the interaction beam-target.

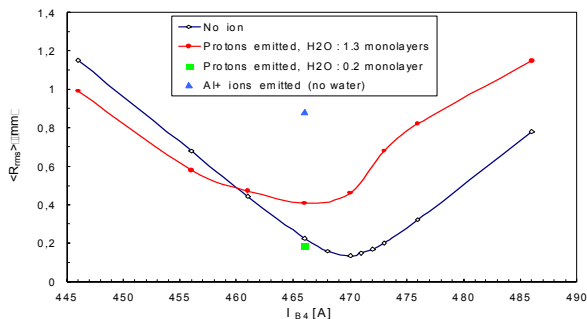


Figure 8: Evolution of the beam rms radius on the target as a function of the current in the last focusing solenoid.

The effect of the different layers (H_2O , Al, Ta) on the target surface has been estimated leading to the evolution of the beam size integrated over the pulse. The evolution of the integrated beam radius has been plotted on Figure 8. It has been shown that the type of atoms and the number of mono-layers have a strong influence on the final beam size.

Modification of the code are made to allow to inject beam particles transported with PARTRAN. In this condition, the pulsed beam is cut transported in slices, each slice being transported independently from the others. This assumption is valid only when the slice length are longer than the beam transverse size.

CONCLUSION

A work is in progress to simulate the full AIRIX accelerator from cathode to target taking into account as much physics as possible. The goal is firstly to be able to predict results observed on the actual machine, and then to propose modifications to increase its performances. We are now able to predict some experimental results at low energy. We have now a simulation tool able to simulate the beam transport from cathode to target, including the diode, an elaborate space-charge routine, a full pulse simulation. The implementation in the simulation tool of the calculus of the beam-target interaction is in progress.

We would like to acknowledge AIRIX team, especially E. Merle and M. Caron for providing us numerous experimental data.

REFERENCES

- [1] E. Merle et al. " Transport of the 1.92 - 3.1 kA AIRIX Electron Beam", PAC 2001, Chicago.
- [2] J. E. Boers, "PBGUNS an interactive IBM PC computer program for the simulation of electron and ion beams and guns", <http://www.thunderbirdsimulations.com>
- [3] <http://www.mrcwdc.com/Magic/index.html>
- [4] R. Duperrier, N. Pichoff, D. Uriot, " CEA Saclay Codes Review for High Intensities Linacs Computations", Proceedings of the International Conference on Computational Science-Part III, pp. 411-418, 2002.
- [5] A. Adolf, "Notice d'utilisation du code M2V", CEA-report, CEA/LV/DMA/MCN DO 2825.
- [6] A. Compant La Fontaine et al., "Emission and Control of H^+ Ions near an Electron-photon Conversion Target", EPAC2002, Paris, France.
- [7] M. Reiser, "Theory and design of charged particle beams", Wiley & son, 1994, (3.131) pp. 93.
- [8] A. Piquemal, O. Mouton, "Modélisation du transport d'un faisceau non-accélééré ...", CEA/DIF/DPTA /SP2A report, DO 10, January 2001.
- [9] L. M. Young, J. H. Billen, "Parmela documentation", LA-UR-96-1835, revised July 17, 2003.
- [10] H. Takeda, J. H. Billen, "Parmila documentation", LA-UR-98-4478, revised January 10, 2004.